Treatment with a global methyltransferase inhibitor induces the intranuclear aggregation of ALS-linked FUS mutant in vitro

（家族性 ALS の原因タンパク質 FUS/TLS に対するメチル化阻害剤の効果）

千葉大学大学院医学薬学府

先端医学薬学専攻

（主任：花澤豊行教授）

今本　早紀子

Treatment with a global methyltransferase inhibitor induces the intranuclear aggregation of ALS-linked FUS mutant in vitro

Sakiko Imamoto

Abstract

FUS/TLS (fused in sarcoma/translocated in liposarcoma) encodes a multifunctional DNA/RNA binding protein with non-classical carboxy (C)-terminal nuclear localization signal (NLS). A variety of ALS-linked mutations are clustered in the C-terminal NLS, resulting in the cytoplasmic mislocalization and aggregation. Since the arginine methylations are implicated in the nuclear-cytoplasmic shuttling of FUS, a methylation inhibitor could be one of therapeutic targets for FUS-linked ALS. We here examined effects of methylation inhibitors on the cytoplasmic mislocalization and aggregates of ALS-linked C-terminal FUS mutant in a cell culture system. Treatment with adenosine dialdehyde (AdOx), a representative global methyltransferase inhibitor, remarkably mitigated the cytoplasmic mislocalization and aggregation of FUS mutant, which is consistent with previous reports. However, AdOx treatment of higher concentration and longer time period evoked the intranuclear aggregation of the ectopic expressed FUS protein. The pull down assay and the morphological analysis indicated the binding between FUS and Transportin could be potentiated by AdOx treatment through modulating methylation status in RGG domains of FUS. These findings indicated the treatment with a methylation inhibitor at the appropriate levels could alleviate the cytoplasmic mislocalization but in excess this could cause the intranuclear aggregation of FUS C-terminal mutant.

Introduction

Amyotrophic lateral sclerosis (ALS) is the most common type of adult motor neuron diseases, characterized by the loss of upper and lower motor neurons. FUS/TLS, one of causative genes for familial ALS and FTLD (Frontotemporal lobar degeneration), encodes a multifunctional DNA/ RNA binding protein, participating in a variety of cellular processes (mRNA splicing, DNA repair, pairing of homologous DNA, cell proliferation, transcriptional regulation, and the transport of mRNAs for local translation in neurites). FUS contains amino (N)-terminal Gln-Gly-Ser- Tyr (QGSY)-rich region and Glycine (G)-rich region, RNA recognition motif (RRM), two Arg-Gly-Gly (RGG) repeats divided by a zinc finger motif, and highly conserved C-terminal non-classical nuclear localization signal (NLS) recognized by Transportin. The majority of ALS-linked mutations of FUS are clustered in the C-terminal NLS, which leads to the cytoplasmic mislocalization [1–6]. N-terminal region, including QGSY and G-rich domain, is a prion-like domain (PrLD) or low complexity (LC) region, which shows prion-like behavior implicated in RNA granules formation [7, 8]. One of primary pathological features in ALS patient is the accumulation of cytoplasmic, ubiquitinated, and insoluble protein aggregates in neurons and glia of the central nervous system. Cytoplasmic aggregation of FUS was reported in ALS cases [1–4, 9], suggesting ‘‘loss of nuclear function’’ and/or ‘‘gain of toxic function’’ could play a role in the etiology of FUS-associated ALS.

Protein arginine methylation is one of post-translational protein modifications. FUS is arginine-methylated by PRMT1 (protein arginine methyltransferase 1) and this could regulate the nuclear-cytoplasmic shuttling of FUS [5, 6, 10–13]. Arginine methylation is catalyzed by PRMTs (protein-arginine-N-methyltransferases), which are generally divided into two categories, type 1 and type 2, based on their arginine methylation patterns. PRMT1 is the major type 1 asymmetric arginine methyltransferase, contributing to *85 % of all cellular PRMT activity utilizing AdoMet (S-adenosyl-L-methionine, or SAM) as the donor of methyl group [14–16]. Thus far, three types of small molecules are known to inhibit the activity of AdoMet-dependent methyltransferases: (1) analogs of AdoMet that compete for the cofactor binding sites, (2) compounds that

disrupt the metabolic loop of AdoMet, (3) specific methyltransferase inhibitors. Among them, adenosine dialdehyde (AdOx) and 5'-methylthioadenosine (MTA) are the most often used as global methyltransferase inhibitors. AdOx, an AdoHcy (S-adenosyl-L-homocystein) hydrolase inhibitor, causes the accumulation of intracellular AdoHcy levels, resulting in the feedback inhibition of most methylation reactions. MTA is also likely to act via AdoMet catabolism. Arginine methylation inhibitor-1(AMI-1), identified by a screening of chemical library, is a small-molecule inhibitor for PRMTs [17–21].

Since the cytoplasmic mislocalization and aggregation of FUS mutant could play a role in the pathogenesis of ALS, a methylation inhibitor might be one of therapeutic targets for FUS-linked ALS. Therefore, it prompted us to examine effects of methylation inhibitors on the mislocalization and aggregates of ALS-linked FUS mutant in a cell culture system.

Materials and Methods

Cell Culture

HEK293 and SH-SY5Y cells were cultured in Dulbecco's modified Eagle's medium (DMEM) supplemented with 10% fetal bovine serum (FBS) at 37°C in a 5% CO_2 atmosphere. Transient transfections were performed using Lipofectamine 2000 (Invitrogen, #11668-027). In some cases, cells were treated with 10–60 μM adenosine-2',3'- dialdehyde (AdOx) (Sigma-Aldrich, #A7154), 100–800 μM 5' -methylthioadenosine (MTA) (Sigma- Aldrich, #D5011) or 100–400 μM AMI-1 (Sigma-Aldrich, #A9232) for 24–48 h and harvested as indicated.

Constructs and Mutagenesis

Human cDNAs for FUS and Transportin 1 were generated by PCR using human cDNA from RIKEN Bioresource Center (Tukuba, Japan) as template. FUS R521G and P525L were generated according to the manual of Quick- Change site-directed mutagenesis kit (Agilent Technologies, #200519). cDNAs for truncated FUS dC (C-terminal NLS deletion mutant) encoding 1-513 aa of FUS and FUS P525L(DRGGs) lacking 370–500 aa region of RGG domains with Zn finger motif were generated by PCR subcloning. The resulting PCR products were subcloned into pAcGFP1 C1 (Clontech), pGEX (GE Healthcare) or FPC1-HA [22] expression vector.

Western Blot Analysis

Western blot analysis was performed as described previously [12, 23]. Cell extracts were prepared by lysis buffer [50 mM Tris–HCl (pH 8.0), 20 mM EDTA, 1 % NP-40, 100 mM NaCl, 10 mM b-glycerophosphate, protease inhibitor cocktail (Roche Diagnostics)]. The samples (30 lg/lane) were boiled in loading buffer [100 mM Tris– HCl (pH 6.8), 200 mM dithiothreitol, 4 % SDS, 0.2 % bromophenol blue, 0.2 % glycerol] for 5 min, and subjected to electrophoresis on 10 % SDS-PAGE. After the proteins were transferred onto polyvinylidene difluoride (PVDF) membrane (Millipore Corp.), the membrane was incubated in blocking buffer [phosphate-buffered saline (PBS) containing 0.05 % Tween 20 (PBS-T) with 5 % nonfat dried milk] for 30 min at room temperature and then probed with a primary antibody in blocking buffer at room temperature for 1 h or overnight at 4 °C. The membrane was washed three times in PBS-T, probed with the secondary horseradish peroxidase-linked anti-mouse or -rabbit IgG antibody (Cell Signaling Biotechnologies) in blocking buffer for 1 h at room temperature, and washed three times in PBS-T. Detection of signal was performed with ECL chemiluminescence system (GE Healthcare Ltd). The primary antibodies used were anti-FUS/TLS (4H11)(Santa Cruz Biotechnologies, sc-47711), anti-Histone H4 (F-9) (Santa Cruz Biotechnologies, sc-25260), anti-GFP (Santa Cruz Biotechnologies, sc-9996), anti-HA (Sigma-Aldrich, HA-7), anti-Actin (I-19) (Santa Cruz Biotechnologies, sc- 1616), and anti-a-Tubulin (B-7) (Santa Cruz Biotechnologies, sc-5286).

Immunocytochemistry

Cells, on cover glass, were fixed with 4 % paraformaldehyde (PFA) for 15 min and then washed three times in PBS. Cells were permeabilized for 5 min in PBS containing 0.2 % Triton X-100 and 5 % bovine serum albumin (BSA), and non-specific sites were blocked by incubating with blocking solution [PBS containing 0.1 % Triton X-100, 5 % BSA]. The cells were incubated with primary antibodies diluted in a blocking solution at room temperature for 1 h or overnight at 4 °C. Then, samples were washed in PBS and incubated with Alexa Fluor 488 (Invitrogen) conjugated secondary antibody for 1 h at room temperature. Then samples were stained with DAPI (4',6- diamino-2-phenylindole) and mounted with a fluorescent mounting medium (DakoCytomation). Images were obtained using fluorescence microscopy (Nikon, E600) equipped with DP72 digital camera.

Pull Down Assay

Pull down assay was performed as described previously [24]. GST fusion proteins were expressed in BL21 Escherichia coli cells, and crude bacterial lysates were prepared by sonication in GST lysis buffer (25 mM Tris at pH 7.5, 150 mM NaCl, 1 mM EDTA, 1 % Triton X-100, protease inhibitor). The lysates were added with 30 µl of glutathione-Sepharose beads (50 % slurry) and mixed for 1 h at 4 °C. The beads were then washed three times with the above GST lysis buffer. Approximately 10 lg of each GST fusion protein was incubated with 100 lg cell extract for 1 h at 4 °C. After the beads were washed three times in GST lysis buffer, proteins from the beads were separated on 10 % SDS-PAGE for Western blotting.

Cell Fractionation Assay

Preparation of cytosolic and nuclear fractions was per- formed as described previously [12]. Briefly, harvested cells from 80 to 90 % confluent culture dish (*1 9 10^7 cells) were suspended in 100 µl Buffer A (10 mM HEPES, pH 7.9, 10 mM KCl, 0.1 mM EDTA, 0.1 mM EGTA, 0.15 % NP-40) containing protease inhibitor and followed by 15 min incubation in 2 ml

eppendorf tube. Homogenates were centrifuged at 12, 000 g for 1 min at 4 °C, and the supernatant (cytosolic fraction) was stored at –80 °C. The pellet, washed with 1 ml Buffer A, was then resuspended in 100 µl Buffer B (20 mM HEPES, pH 7.9, 0.4 mM NaCl, 1 mM EDTA, 1 mM EGTA, 0.5 % NP-40) containing protease inhibitor and sonicated at 4 °C. Cellular debris was removed by centrifugation at 12,000 g for 30 min at 4 °C and the supernatant (nuclear fraction) was stored at -80 °C.

Quantification for Western Blot Bands

Western blot images were analyzed with ImageJ software (National Institutes of Health), which evaluates the relative amount of protein staining with normalization to the corresponding controls.

Statistical Analysis

Quantitative data were analyzed by the Student's t test for two groups or one-way analysis of variance (ANOVA) with post hoc statistical analysis for three or more group comparisons, with p values less than 0.05 considered as statistically significant. Data were expressed as means ± standard errors (SE).

Results

Subcellular Localization of ALS-Linked Mutants in SH-SY5Y and HEK293

To examine the subcellular localization of ALS-linked FUS mutants, we generated plasmids encoding GFP-tagged FUS wild type (wt), FUS R521G, FUS P525L, and FUS dC (Fig. 1a). FUS P525L, with the mutation in C-terminal PY domain recognized by Transportin, causes the severe phenotype in the patients [6, 25]. FUS R521G patients show relatively moderate phenotype compared with those of FUS P525L [2]. FUS dC (1-513 amino acid) lacks the C-terminal NLS (514–526 aa), which is comparable to FUS R495X (truncation of C-terminal NLS) [26]. We then examined the subcellular localization of FUS mutants using neuronal SH-

SY5Y and non-neuronal cell line HEK293. SH-SY5Y and HEK293 cells were transiently transfected with each plasmid and then fixed at 24 h after transfection. In SH-SY5Y cells, FUS wt was exclusively located in the nucleus, while FUS R521G was observed mainly in the nucleus with weak cytoplasmic signals (Fig. 1b). FUS P525L and FUS dC were localized both in the nucleus and cytoplasm with cytoplasmic granules (*1 μm) (Fig. 1b, c). Approximately 10 % of cells transfected with FUS P525L or FUS dC spontaneously formed large aggregates ([5 μm) in SH-SY5Y (Fig. 1b, c) as previously described [27]. The cell types in SH-SY5Y were categorized into four subclasses, including ‘‘Nucleus’’, ‘‘Diffused’’, ‘‘Granules’’, and ‘‘Aggregates’’ type (Fig. 1c). In contrast to SH-SY5Y, cytoplasmic aggregates were formed in most of cells expressing GFP-FUS R521G, FUS P525L, and FUS dC in HEK293 (Fig. 1d). The cell types in HEK293 were also categorized into four subtypes, including ‘‘Nucleus’’, ‘‘Nucleus and Cytoplasm (N +C)’’, ‘‘Nucleus and Aggregates (N + Aggre), and ‘‘Aggregates dominant (Aggregates)’’ type (Fig. 1e).

To rule out the effect of GFP protein, we generated plasmids encoding HA-tagged FUS wt and each mutant and examined the subcellular localizations. SH-SY5Y and HEK293 cells, transfected with plasmid encoding HA-tagged FUS wt or each mutant, indicated the similar distribution patterns to those of GFP-FUS-transfected cells (Supplementary Fig. 1A). In addition, the expression levels of ectopic expressed FUS protein in HEK293 (transfection efficiency is *80 %) were approximately 1–1.8 fold compared with those of endogenous FUS protein (Supplementary Fig. 1B).

Effects of Methylation Inhibitors on the Subcellular Localization of FUS P525L

Previous reports have shown the inhibition of arginine methylation restores Transportin-mediated nuclear import of ALS-associated FUS mutant [5, 6]. To examine effects of various methylation inhibitors on the subcellular localization, SH-SY5Y and HEK293 cells over-expressing GFP-FUS P525L were treated with two global methyltransferase inhibitors (AdOx and MTA) and a specific PRMTs inhibitor (AMI-1). Cells, transiently transfected with FUS P525L plasmid, were treated with each inhibitor for 24 h initiating at 12 h after transfection. AdOx treatment at the

concentration of 20 μM dramatically reduced the cytoplasmic mislocalization in both cell lines (Fig. 2a), which is consistent with the previous report [6]. We then examined the effects of AdOx on the cytoplasmic aggregates that were observed in HEK293. As shown in Fig. 2b, 10–20 μM AdOx treatment reduced the ratio of cells with cytoplasmic aggregates in a dose-dependent manner in HEK293. Interestingly, AdOx treatment at higher concentration of 60 μM induced the intranuclear aggregation of FUS P525L in HEK 293 (21 ± 4 % of transfected cells) and SH-SY5Y (16 ± 2 % of transfected cells) (Fig. 2a). We confirmed these aggregates actually located in the nucleus by confocal laser scanning microscopy (Supplementary video). Furthermore, AdOx treatment also evoked the intranuclear aggregation of GFP-fused FUS wt and HA-tagged FUS wt in HEK293 (Supplementary Fig. 1C).

To rule out the effect of GFP, we then examined the effects of AdOx treatment on the subcellular localization of GFP alone and HA-tagged FUS P525L. The treatment had no effect on the subcellular localization of GFP (Supplementary Fig. 2A) and indicated the similar effects on HA- tagged FUS P525L to those on GFP-FUS P525L (Supplementary Fig. 2B). Although MTA and AMI-1 are reportedly effective at the concentration of *800 and *400 μM respectively [21, 28], either had little effect on the cyto-plasmic mislocalization of FUS P525L morphologically both in HEK293 and SH-SY5Y (Fig. 2c; Supplementary Fig. 2C). To quantify these effects, HEK293 cells over- expressing FUS P525L were treated with mock, AdOx, or MTA and then processed for subcellular fractionation assay. Since the transfection efficiency in HEK293 (*80 %) is much higher than that in SH-SY5H (*20 %), we used HEK293 for the following biochemical assays. AdOx treatment increased Nuclear/Cytosol ratio of FUS P525L compared with that of Mock, suggesting the treatment reduced the cytoplasmic mislocalization [N/C ratio; FUS wt, 6.5 ± 1.9; P525L (Mock), 1.8 ± 0.12; P525L (AdOx); 3.2 ± 0.59; P525L (MTA), 2.2 ± 0.48] (Fig. 2d). There were small molecular weight bands in the lane of FUS P525L in Fig. 2d. Since FUS protein undergoes various post-translational modifications including methylation and phosphorylation [6, 7, 10], those bands could partly be due to the changes in protein modifications as a result of cytoplasmic mislocalization.

Additionally to confirm effects of methylation inhibitors used in the present study, we performed methylation assays using the antibody to detect methylated arginines. HEK293 cells were treated with each inhibitor for 24 h and processed for methylation assays. As in Supplementary Fig. 2D, all the methylation inhibitors used in the present study actually mitigated the levels of arignine methylation of FUS by 40–60 %.

The arginine methylation in the RGG domain of FUS impairs the binding of Transportin in pull down assays using the peptides of FUS RGG domain [6]. Using whole cell lysates pretreated with AdOx in pull down assay, we here examined whether the methylation inhibitor regulates the binding between FUS and Transportin1. GST-fused Transportin1 (GST-TRN) was bacterially generated and incubated with HEK293 lysates pretreated with 20 μM AdOx for 24 h. The band intensity showing the binding between FUS and GST-TRN was increased by AdOx pretreatment (Fig. 2e). Then to investigate whether argi- nine methylations in RGG domains next to C-terminal NLS (Fig. 1a) are critical for the binding between FUS and Transportin1, we generated plasmid encoding GFP-FUS P525L (DRGGs) that lacks RGG domains (370–500 aa). SH-SY5Y cells, transfected with the plasmid, were treated with 20 μM AdOx for 24 h. AdOx treatment had no effect on the subcellular localization of GFP-FUS P525L (DRGGs) (Fig. 2f), suggesting RGG domains of FUS might be important for effects of AdOx treatment as described previously [6].

Timing of AdOx Treatment is Critical for its Effects

Using neuronal SH-SY5Y cells, we then examined whether the time point and/or time period of AdOx application are critical for its effects on the mislocalization of FUS P525L in vitro. SH-SY5Y cells, transiently transfected with GFP- FUS P525L plasmid, were treated with mock or 20 μM AdOx for 24 h initiating at 12, 24, and 36 h after transfection (Fig. 3a). The effects of AdOx treatment were apparently decreased when applied at 36 h after plasmid transfection. To quantify these results, we categorized cells into two distribution types of FUS-P525L, ‘‘N (nucleus)’’ and ‘‘N＋C (nucleus plus cytoplasm)’’ and estimated the ratio of each type. The percentages of ‘‘N’’ type cells recovered by 24 h AdOx treatment were

decreased in a time-dependent manner (Fig. 3b), suggesting the time point of AdOx application is critical for its effects in vitro.

We then notified even 20 μM Adox treatment induced the intranuclear aggregates of FUS P525L to some extent, which apparently is dependent on the duration of AdOx treatment. To quantify this, SH-SY5Y cells expressing GFP-FUS P525L were treated with 20 μM AdOx for 24, 36, or 48 h initiating at 12 h after plasmid transfection. AdOx treatment of longer time periods increased the percentage of cells with intranuclear aggregates in a time-dependent manner as shown in Fig. 3c. Taken together, various factors including the concentration and the timing of AdOx treatment might be critical for its effects on the mislocalization and aggregation of FUS P525L in vitro.

Discussion

Since a methylation inhibitor could be one of therapeutic targets for FUS-linked ALS, we examined effects of two global methyltransferase inhibitors (AdOx and MTA) and one specific PRMTs inhibitor (AMI-1) on the cytoplasmic mislocalization and aggregation of FUS-P525L in vitro. 20 μM AdOx treatment for 24 h initiating at 12–24 h after transfection remarkably mitigated the cytoplasmic mislocalization, while another global methyltransferase inhibitor MTA and a specific PRMTs inhibitor AMI-1 had little effect morphologically. The pull down assay and the morphological analysis with FUS deletion mutant [FUS P525L (DRGGs)] suggested AdOx treatment could potentiate the binding between FUS and Transportin through modulating the methylation status in RGG domains, which are consistent with the previous reports [5, 6].

In response to various stresses, ALS-linked FUS mutants are assembled into stress granules in proportion to the cytoplasmic expression levels and that prolonged stress could trigger aggregation of ‘pathological’ stress granules, which possibly leads to the disruption of RNA metabolism [27, 29, 30]. Therefore, reducing the mislocalization of FUS mutant could be one of promising therapeutic strategies for FUS-related ALS. Based on the

present results, AdOx treatment at the appropriate concentration and timing was remarkably effective on the cytoplasmic mislocalization and aggregation. Since global methyltransferase inhibitors including AdOx inhibit most of methylation reactions using AdoMet as the donor, specific PRMTs inhibitors could be ideal therapeutic candidates. Unfortunately AMI-1, a specific PRMTs inhibitor, had little effect in the present study. The effect on the relocalization of SMN (Survival of Motor Neuron) was observed only with MTA but not with Adox treatment [28], suggesting some additional factors might be implicated in these phenomena.

N-terminal region corresponding to SQGY and G-rich domain is prion-like domain (PrLD) or low-complexity (LC) sequence, which can reversibly transform to a polymeric amyloid-like state [7, 8]. We assumed the protein concentration levels of FUS in the nucleus could be one of critical factors for AdOx-induced intranuclear aggregates because the percentage of cells with intranuclear aggregation increased in a time-dependent manner after AdOx treatment (Fig. 3c). The intranuclear aggregates were presumably formed once FUS protein levels in the nucleus exceed the threshold with AdOx treatment. Recently it was shown FUS autoregulates its own protein levels through modulating its own alternative splicing [31]. Especially, the cytoplasmic mislocalization of C-terminal FUS mutant could lead to the deficiency of this autoregulation and the enhanced expression levels of FUS protein [31]. In addition, Schwartz et al. [32] has shown that FUS is trapped in the nuclear aggregates in fibroblasts of ALS patients with FUS C-terminal mutants, which altered distribution and Ser-2 phosphorylation of RNA Polymerase II and might affect the transcription of many genes. Taken together, these findings raise the possibility the treatment with a methylation inhibitor could evoke the intranuclear aggregation of FUS C-terminal mutant in vivo and this could leads to the impairment of gene transcription.

In summary, the treatment with a methylation inhibitor at appropriate levels could alleviate the cytoplasmic mis- localization of FUS C-terminal mutant in vitro, which might be one of promising approaches for FUS-linked ALS. However, in excess this could result in the intranuclear aggregation of FUS mutant.

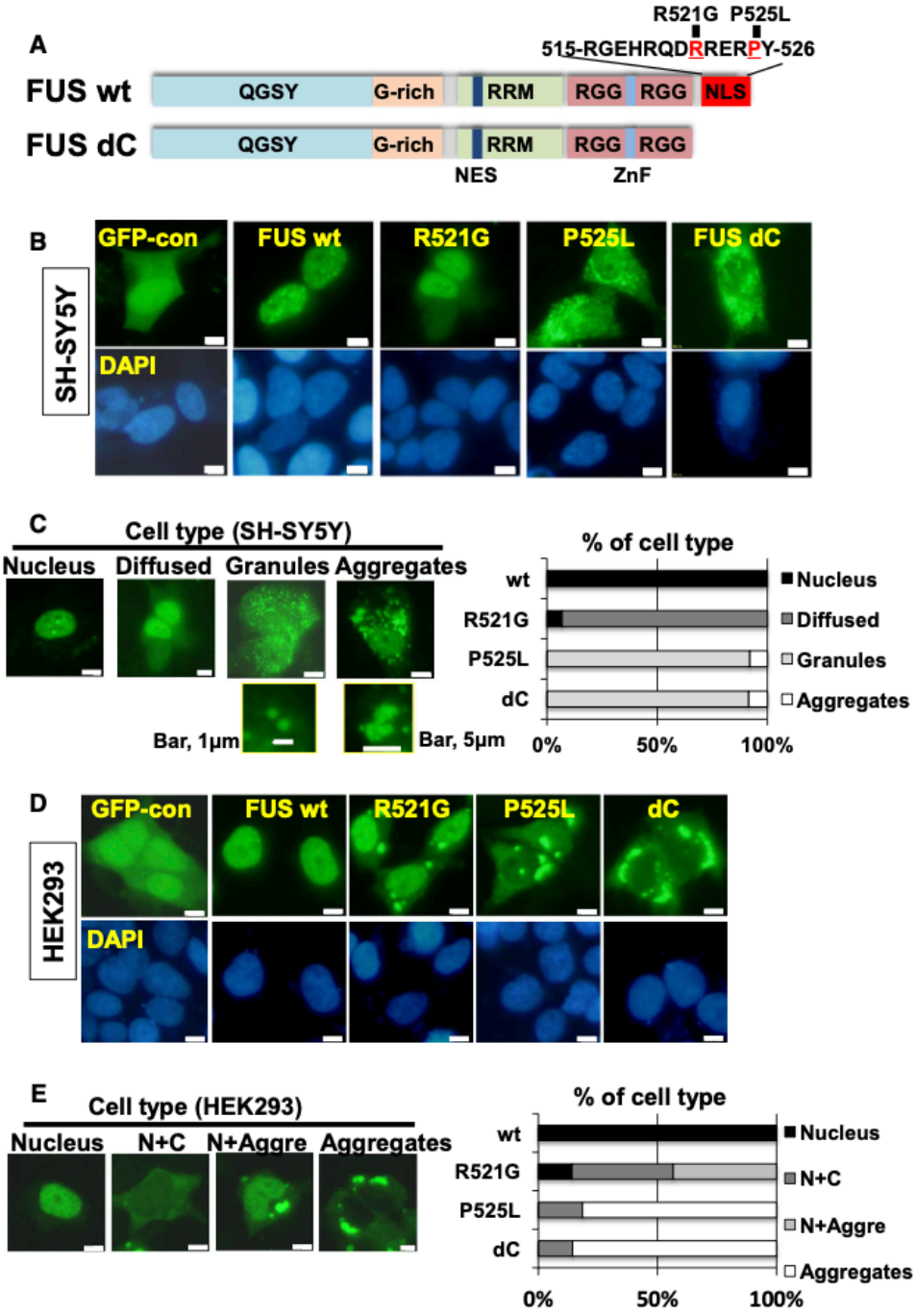

Fig. 1 Subcellular localization of GFP-FUS mutant in SH- SY5Y and HEK293.

a Diagrams representing FUS wild type (FUS wt), missense mutations (FUS R521G and FUS P525L), and C-terminal NLS deletion mutant (FUS dC). QGSY, Gln-Gly-Ser-Tyr-rich region; G-rich, Gly-rich region; RRM,

RNA recognition motif; NES, nuclear export signal; RGG, Arg-Gly-Gly repeats; ZnF, zinc finger domain; NLS, nuclear localization signal.

b, d SH-SY5Y and HEK293 cells, transiently transfected with GFP control (GFP-con), GFP-fused FUS wt, FUS R521G, FUS P525L, or FUS dC plasmid, were fixed at 24 h after transfection and then stained with DAPI (diamidino-2- phenylindole). Images were obtained using fluorescence microscopy. Bars, 5 μm.

c, e SH-SY5Y and HEK293 cells, transfected with each GFP-FUS plasmid, were categorized into subtypes (left panels) and represented as % ratio in bar graph (right graph). For the categorizations, total 120 cells (40 cells/each assay) were counted in three independent experiments. Bars, 5 μm.

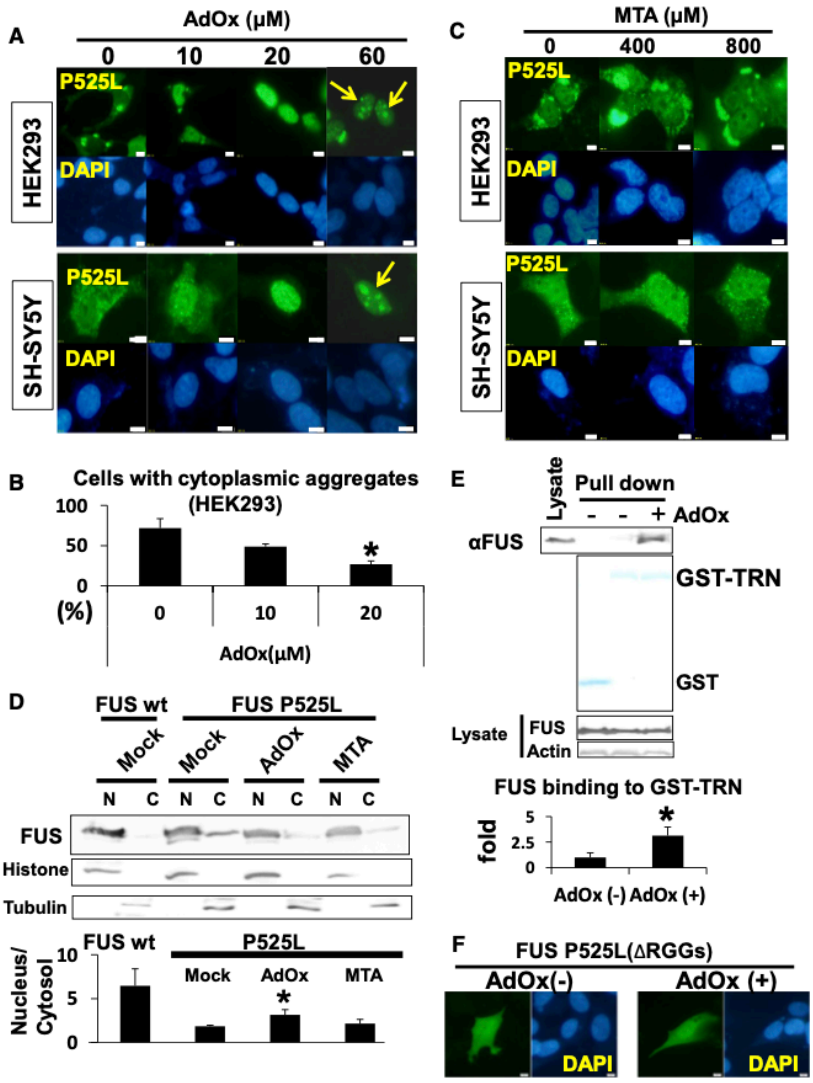

Fig. 2 Effects of methylation inhibitors on the mislocalization of GFP-FUS P525L.

a, c HEK293 and SH-SY5Y cells, transiently transfected with GFP-FUS P525L plasmid, were treated with AdOx (0, 10, 20, 60 μM) and MTA (0, 400, 800 μM), respectively, for 24 h initiating at 12 h after transfection. Cells were fixed and then stained with DAPI. Images were obtained using fluorescence microscopy. Arrows in Fig. 2a (AdOx 60 μM) indicate the intranuclear aggregates. Bars, 5 μm.

b Graph represents % ratio of HEK293 cells with cytoplasmic aggregates per transfected cells when treated with 0, 10, or 20 μM AdOx for 24 h. For

the quantification, total 120 cells (40 cells/each assay) were counted in three independent experiments. Quantitative data were analyzed by one-way analysis of variance (ANOVA) with post hoc statistical analysis. Asterisk (*) represents p value <0.05 versus AdOx 0 μM.

d HEK293 cells, transiently transfected with HA-tagged FUS wt or FUS-P525L plasmid, were treated with mock, AdOx (20 μM), or MTA (800 μM) for 24 h initiating at 12 h after transfection. Then cells were processed for subcellular fractionation assays. Aliquots (20 μg) of each extracts were separated on 10 % SDS-PAGE and subjected to the immuno- blots with anti-HA (top), -Histone (middle), and -Tubulin (bottom panel) antibody. ‘‘N’’ and ‘‘C’’ means nuclear and cytosolic fraction, respectively. Bar graph represents averaged data of Nucleus/Cytosol ratio of FUS P525L, expressed as mean ± SE of 3 separate experiments. ‘‘Nucleus/Cytosol ratio’’ was calculated as relative intensities in nuclear fraction over those in cytosolic fraction. Quantitative data were analyzed by one-way analysis of variance (ANOVA) with post hoc statistical analysis. Asterisk (*) represents p value <0.05 versus Mock.

e GST-cont and GST-TRN (10 μg each) were bacterially produced, and incubated with HEK293 lysates (100 μg) pretreated with Mock (AdOx -) or AdOx (AdOx+) for 24 h. After washing, samples were subjected to Western blotting with anti-FUS antibody (upper panel). The lower panel shows the Coomassie brilliant blue (CBB)-stained SDS-polyacrylamide gel with GST fusion proteins used in the pull-down experiment. Lysates of the samples (30 μg/well) were immunoblotted with the indicated antibodies (bottom panels). Bottom graph indicates the band intensities of FUS protein binding to GST-TRN, treated with Mock (AdOx -) and AdOx (AdOx +) (n = 3, mean ± SE). Quantitative data were analyzed by the Student’s t test. Asterisk (*) represents p value <0.05 versus Mock. (F) SH-SY5Y cells, transiently transfected with GFP- tagged FUS P525L (DRGGs) plasmid, were treated with (+) or without (-) 20 μM AdOx for 24 h initiating at 12 h after transfection and then fixed for observation with fluorescence microscopy. Samples were stained with DAPI. Bars, 5 μm.

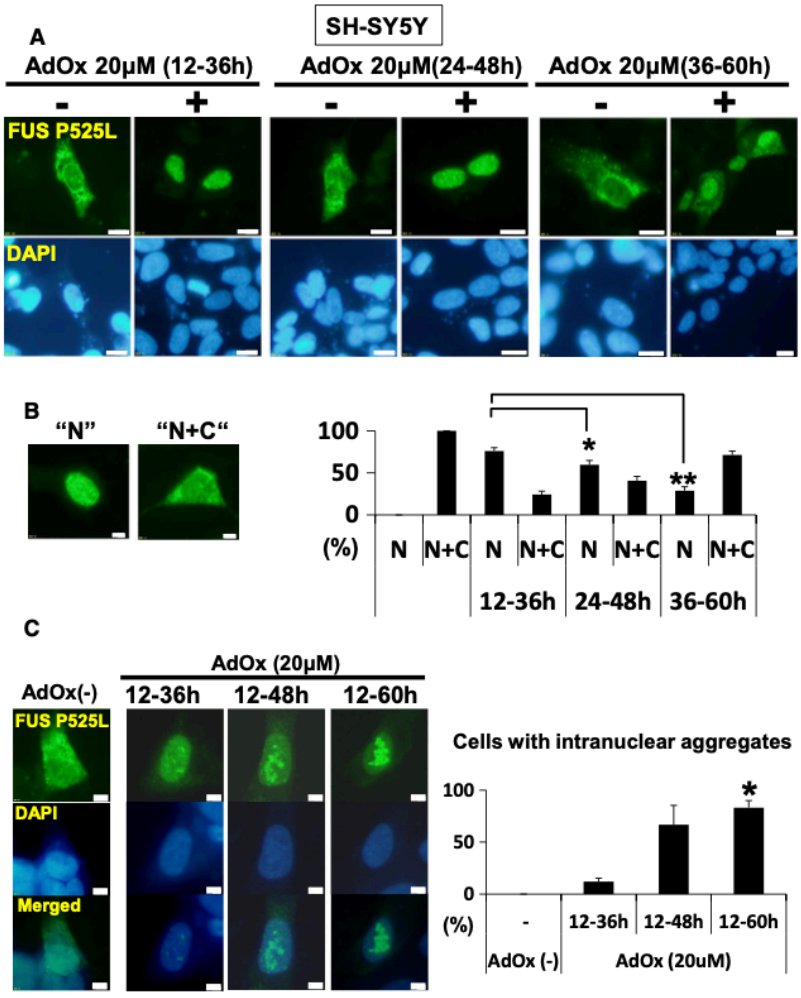

Fig. 3 Timing of AdOx treatment is critical for its effects.

a SH- SY5Y cells, transiently transfected with GFP-FUS P525L plasmid, were treated with (+) or without (-) 20 μM AdOx for 24 h for the indicated time periods after transfection. After treatment, cells were fixed and stained with DAPI. Bars, 10 μm.

b Left pictures indicate the cell type of SH-SY5Y cell, harboring signals of FUS P525L only in the nucleus (‘‘N’’) or both in the nucleus and cytoplasm (‘‘N + C’’). Right graph shows % ratio of SH-SY5Y cell with ‘‘N’’ and ‘‘N +C’’ type, with AdOx treatments for the indicated time periods after transfection. At least 40 cells per each experiment were counted in triplicate (n = 3, mean ± SE). Quantitative data were analyzed by one-way analysis of variance (ANOVA) with post hoc statistical

analysis. Asterisks (*, **) represent p value <0.05 compared with AdOx treatment (12–36 h). Bars, 5 μm.

c SH-SY5Y cells, transiently transfected with GFP-FUS P525L plasmid, were treated with 20 μM AdOx for the indicated time periods after transfection. Then cells were fixed and stained with DAPI. Bars, 2 μm. Right graph shows % ratio of cells with intranuclear aggregates per transfected cells. At least 40 cells per each experiment were counted in triplicate (n = 3, mean ± SE). Quantitative data were analyzed by one-way analysis of variance (ANOVA) with post hoc statistical analysis. Asterisk (*) represents p value <0.05 versus AdOx treatment (12–36 h) .

References

1. Vance C, Rogelj B, Hortobagyi T, De Vos KJ, Nishimura AL, Sreedharan J, Hu X, Smith B, Ruddy D, Wright P, Ganesalingam J, Williams KL, Tripathi V, Al-Saraj S, Al-Chalabi A, Leigh PN, Blair IP, Nicholson G, de Belleroche J, Gallo JM, Miller CC, Shaw CE (2009) Mutations in FUS, an RNA processing protein, cause familial amyotrophic lateral sclerosis type 6. Science 323:1208–1211
2. Kwiatkowski TJ Jr, Bosco DA, Leclerc AL, Tamrazian E, Vanderburg CR, Russ C, Davis A, Gilchrist J, Kasarskis EJ, Munsat T, Valdmanis P, Rouleau GA, Hosler BA, Cortelli P, de Jong PJ, Yoshinaga Y, Haines JL, Pericak-Vance MA, Yan J, Ticozzi N, Siddique T, McKenna-Yasek D, Sapp PC, Horvitz HR, Landers JE, Brown RH Jr (2009) Mutations in the FUS/TLS gene on chromosome 16 cause familial amyotrophic lateral sclerosis. Science 323:1205–1208
3. Lagier-Tourenne C, Cleveland DW (2009) Rethinking ALS: the FUS about TDP-43. Cell 136:1001–1004
4. Lagier-Tourenne C, Polymenidou M, Cleveland DW (2010) TDP-43 and FUS/TLS: emerging roles in RNA processing and neurodegeneration. Hum Mol Genet 19:R46–R64
5. Dormann D, Rodde R, Edbauer D, Bentmann E, Fischer I, Hruscha A, Than ME, Mackenzie IR, Capell A, Schmid B, Neumann M, Haass C

(2010) ALS-associated fused in sarcoma (FUS) mutations disrupt Transportin-mediated nuclear import. EMBO J 29:2841–2857
6. Dormann D, Madl T, Valori CF, Bentmann E, Tahirovic S, Abou-Ajram C, Kremmer E, Ansorge O, Mackenzie IR, Neumann M, Haass C (2012) Arginine methylation next to the PY-NLS modulates Transportin binding and nuclear import of FUS. EMBO J 31:4258–4275
7. Kato M, Han TW, Xie S, Shi K, Du X, Wu LC, Mirzaei H, Goldsmith EJ, Longgood J, Pei J, Grishin NV, Frantz DE, Schneider JW, Chen S, Li L, Sawaya MR, Eisenberg D, Tycko R, McKnight SL (2012) Cell-free formation of RNA granules: low complexity sequence domains form dynamic fibers within hydrogels. Cell 149:753–767
8. Kwon I, Kato M, Xiang S, Wu L, Theodoropoulos P, Mirzaei H, Han T, Xie S, Corden JL, McKnight SL (2013) Phosphorylation- regulated binding of RNA polymerase II to fibrous polymers of low-complexity domains. Cell 155:1049–1060
9. Mackenzie IR, Rademakers R, Neumann M (2010) TDP-43 and FUS in amyotrophic lateral sclerosis and frontotemporal dementia. Lancet Neurol 9:995–1007
10. Du K, Arai S, Kawamura T, Matsushita A, Kurokawa R (2011) TLS and PRMT1 synergistically coactivate transcription at the survivin promoter through TLS arginine methylation. Biochem Biophys Res Commun 404:991–996
11. Tradewell ML, Yu Z, Tibshirani M, Boulanger MC, Durham HD, Richard S (2012) Arginine methylation by PRMT1 regulates nuclear-cytoplasmic localization and toxicity of FUS/TLS har- bouring ALS-linked mutations. Hum Mol Genet 21:136–149
12. Yamaguchi A, Kitajo K (2012) The effect of PRMT1-mediated arginine methylation on the subcellular localization, stress granules, and detergent-insoluble aggregates of FUS/TLS. PLoS One 7:e49267
13. Scaramuzzino C, Monaghan J, Milioto C, Lanson NA Jr, Maltare A, Aggarwal T, Casci I, Fackelmayer FO, Pennuto M, Pandey UB (2013) Protein arginine methyltransferase 1 and 8 interact with FUS to modify its sub-cellular distribution and toxicity in vitro and in vivo. PLoS One 8:e61576

14. Lee HW, Kim S, Paik WK (1977) S-adenosylmethionine: pro- tein-arginine methyltransferase. Purification and mechanism of the enzyme. Biochemistry 16:78–85
15. Nicholson TB, Chen T, Richard S (2009) The physiological and pathophysiological role of PRMT1-mediated protein arginine methylation. Pharmacol Res 60:466–474
16. Bedford MT, Clarke SG (2009) Protein arginine methylation in mammals: who, what, and why. Mol Cell 33:1–13
17. Cheng D, Yadav N, King RW, Swanson MS, Weinstein EJ, Bedford MT (2004) Small molecule regulators of protein arginine methyltransferases. J Biol Chem 279:23892–23899
18. Wang J, Chen L, Sinha SH, Liang Z, Chai H, Muniyan S, Chou YW, Yang C, Yan L, Feng Y, Li KK, Lin MF, Jiang H, Zheng YG, Luo C (2012) Pharmacophore-based virtual screening and biological evaluation of small molecule inhibitors for protein arginine methylation. J Med Chem 55:7978–7987
19. Williams-Ashman HG, Seidenfeld J, Galletti P (1982) Trends in the biochemical pharmacology of 5’-deoxy-5’-methylthioadeno- sine. Biochem Pharmacol 31:277–288
20. Osborne TC, Obianyo O, Zhang X, Cheng X, Thompson PR (2007) Protein arginine methyltransferase 1: positively charged residues in substrate peptides distal to the site of methylation are important for substrate binding and catalysis. Biochemistry 46:13370–13381
21. Bonham K, Hemmers S, Lim YH, Hill DM, Finn MG, Mowen KA (2010) Effects of a novel arginine methyltransferase inhibitor on T-helper cell cytokine production. FEBS J 277:2096–2108
22. Endo M, Ohashi K, Mizuno K (2007) LIM kinase and slingshot are critical for neurite extension. J Biol Chem 282:13692–13702 23.
23. Koga S, Kojima S, Kishimoto T, Kuwabara S, Yamaguchi A (2012) Over-expression of map kinase phosphatase-1 (MKP-1) suppresses neuronal death through regulating JNK signaling in hypoxia/re-oxygenation. Brain Res 1436:137–146
24. Chen Y, Zhang L, Jones KA (2011) SKIP counteracts p53-mediated apoptosis via selective regulation of p21Cip1 mRNA splicing. Genes Dev 25:701–716

25. Conte A, Lattante S, Zollino M, Marangi G, Luigetti M, Del Grande A, Servidei S, Trombetta F, Sabatelli M (2012) P525L FUS mutation is consistently associated with a severe form of juvenile amyotrophic lateral sclerosis. Neuromuscul Disord 22:73–75
26. Bosco DA, Lemay N, Ko HK, Zhou H, Burke C, Kwiatkowski TJ Jr, Sapp P, McKenna-Yasek D, Brown RH Jr, Hayward LJ (2010) Mutant FUS proteins that cause amyotrophic lateral sclerosis incorporate into stress granules. Hum Mol Genet 19:4160–4175
27. Takanashi K, Yamaguchi A (2014) Aggregation of ALS-linked FUS mutant sequesters RNA binding proteins and impairs RNA granules formation. Biochem Biophys Res Commun 452: 600–607
28. Boisvert FM, Cote J, Boulanger MC, Cleroux P, Bachand F, Autexier C, Richard S (2002) Symmetrical dimethylarginine methylation is required for the localization of SMN in Cajal bodies and pre-mRNA splicing. J Cell Biol 159:957–969
29. Gal J, Zhang J, Kwinter DM, Zhai J, Jia H, Jia J, Zhu H (2011) Nuclear localization sequence of FUS and induction of stress granules by ALS mutants.Neurobiol Aging 32(12):2323.e27-40
30. Buratti E, Baralle FE (2012) TDP-43: gumming up neurons through protein-protein and protein-RNA interactions. Trends Biochem Sci 37:237–247
31. Zhou Y, Liu S, Liu G, Ozturk A, Hicks GG (2013) ALS-associated FUS mutations result in compromised FUS alternative splicing and autoregulation. PLoS Genet 9:e1003895
32. Schwartz JC, Podell ER, Han SS, Berry JD, Eggan KC, Cech TR (2014) FUS is sequestered in nuclear aggregates in ALS patient fibroblasts. Mol Biol Cell 25:2571–2578

Neurochemical Research Vol. 41 No.4
2015 年 11 月 24 日公表済
DOI 10.1007/s11064-015-1758-z